Investigation of the structure of the relaxor ferroelectric $Pb(Fe_{1/2}Nb_{1/2})O_3$ by neutron powder diffraction

Investigation of the structure of the relaxor ferroelectric Pb(Fe$_{1/2}$Nb$_{1/2}$)O$_3$ by neutron powder diffraction

Sergey A Ivanov†‖, Roland Tellgren‡, Häkan Rundlof‡, Noel W Thomas§¶ and Supon Ananta§

† Department of Inorganic Materials, Karpov' Institute of Physical Chemistry, Ul. Vorontsovo Pole, 103064 Moscow K-64, Russia
‡ Department of Inorganic Chemistry, Ångstrom Laboratory, Box 538, University of Uppsala, SE-751 21, Uppsala, Sweden
§ Department of Materials, University of Leeds, Leeds LS2 9JT, UK

E-mail: `ivan@cc.nifhi.ac.ru` and `rte@studsvik.uu.se` and `nthomas@wbb.co.uk`

Abstract.   The complex perovskite lead iron niobate, Pb(Fe$_{1/2}$Nb$_{1/2}$)O$_3$ (PFN), has been studied by neutron powder diffraction. Following collection of diffraction data at 300 K and at 10 K, structural refinements have been carried out by means of the Rietveld method. As expected, a straightforward unit cell of symmetry $R3m$ was obtained for the 300 K structure, with the same symmetry and a similar unit cell also obtained at low temperature. Furthermore, in order to obtain a good agreement with experiment at 10 K, it was necessary to assign non-zero magnetic moments to the iron ions, these being in a collinear, antiferromagnetic alignment. This magnetic structure can be described with reference to doubled unit cell axes. The factors governing the observed structures of PFN are discussed by comparison with the related system of Pb(Mg$_{1/3}$Nb$_{2/3}$)O$_3$.

1. Introduction

Lead iron niobate (Pb(Fe$_{1/2}$Nb$_{1/2}$)O$_3$; PFN) is well known as a lead-based complex perovskite with ferroelectric properties. It is currently of interest as a component in commercial electroceramic materials, particularly as it is typically characterized by high relative permittivities and low sintering temperatures.

Since there are only a few articles devoted to PFN itself, whether in single crystal [1–3] or ceramic form [4–6], the focus here is to examine the crystal structure of this material, both at 300 K and at 10 K. Although PFN is generally thought to have polar rhombohedral $R3m$ symmetry at room temperature, undergoing a diffuse phase transition at 387 K to cubic $Pm3m$ symmetry [7], more recent work on single crystals has suggested a small monoclinic distortion away from rhombohedral symmetry at room temperatures, together with the existence of an intermediate phase of tetragonal symmetry at temperatures between 355 K and the ferroelectric Curie point of 376 K [3]. Moreover, antiferromagnetic G-type spin ordering has been found in powder PFN samples at temperatures below 143 K [8, 9].

Since the symmetries of the non-cubic phases of PFN are still open to debate [3, 10–13], a neutron powder diffraction study of the kind presented here is timely and also relevant to

‖ Author to whom correspondence should be addressed.
¶ Present address: WBB Technology Ltd, Watts Blake Bearne & Co. Plc, Park House, Courtenay Park, Newton Abbot TQ12 4PS, UK.

the wider aim of gaining a better understanding of the structures of lead-based perovskite ferroelectrics, amongst which relaxor properties are prevalent. By comparison with XRD, neutron powder diffraction is able to provide more accurate information on the positions of the oxygen ions. It is these which essentially determine the space group symmetry and order parameters of the phase transitions. A further advantage of studying the PFN system by this technique is that unique insight may be gained into the relationship between ferroelectric and magnetic properties.

2. Experiment

Single-phase PFN powders were prepared by an optimized two-step calcination method involving columbite-like $FeNbO_4$ intermediates [14, 15]. Neutron powder diffraction (NPD) data were collected at the Swedish Research Reactor R2 in Studsvik, by means of a Huber two-circle diffractometer with an array of 35 ^{3}He detectors. The monochromator system used two parallel copper crystals in (220) mode, giving rise to a wavelength of 1.470 Å. The neutron flux at the sample position was approximately 10^6 neutrons cm^{-2} s^{-1}. Data were collected at 300 K and 10 K from powdered samples of PFN (approximately 5 g) loaded into a vanadium container, with detector intensities statistically analysed and summed. Corrections for absorption effects were subsequently carried out in the Rietveld refinements, utilizing the empirical value $\mu R = 0.074$ cm^{-1}. The step scan covered the 2θ range 4–139.5° with step size 0.05°.

Diffraction datasets were refined by the Rietveld method using FULLPROF software [16], with neutron scattering lengths obtained from the literature [17]. The magnetic form factor adopted for Fe was identical to that tabulated in the FULLPROF program. Diffraction peaks were described by a pseudo-Voigt function, with a Lorentzian contribution to the Gaussian peak shape refined. A peak asymmetry correction was made for angles below 35° 2θ. Background intensities were described by a polynomial with six coefficients, which were refined simultaneously with one scale factor. One additional parameter was included in the refinement of the low temperature phase, in order to allow variations in magnitude of the magnetic moments in an antiferromagnetic arrangement.

3. Results

Analysis of the neutron diffraction data confirmed that the cationic stoichiometry and oxygen content were in agreement with the existence of a single phase of the proposed composition, i.e. $Pb(Fe_{1/2}Nb_{1/2})O_3$. The cationic stoichiometric coefficients were within ∼0.01 of their idealized values, and the oxygen content determined as 3.00, with a calculated standard error of 1%. Further, the refined atomic ratio of Nb:Fe was very close to unity.

The NPD pattern at 300 K was refined in space group $R3m$ (in hexagonal axes), with Fe and Nb atoms assumed to occupy 3a sites randomly. No extra peaks or additional splitting of main reflections were observed. The final structural parameters from this refinement are given in table 1, with a good agreement between the experimental diffraction pattern and calculated profile indicated in figure 1. An interpretation of the large value of the isothermal temperature factor, B, for the lead cation is given in the following section.

Refinement of the NPD data collected at 10 K was also carried out in the space group $R3m$. However, additional peaks were observed in the 10 K diffraction patterns, which could not be accommodated by assuming a reduction from rhombohedral to monoclinic crystal symmetry (figure 2). Given that PFN has been found to exhibit antiferromagnetic

Table 1. Rhombohedral structure of PFN at 300 K. Space Group $R3m$; cell parameters in table 3.

Atom	Point symmetry	x	y	z	B (Å^2)
With respect to hexagonal axes					
Pb	3a	0	0	0	2.33(5)
Nb/Fe	3a	0	0	0.4860(9)	0.20(4)
O	9b	0.1745(6)	−0.1745(6)	0.3367(9)	1.18(4)
With respect to rhombohedral (pseudo-cubic) axes					
Pb	1a	0.012(2)	0.012(2)	0.012(2)	3.09(11)
Nb/Fe	1a	0.5	0.5	0.5	0.20(4)
O	3b	0.5256(5)	0.5256(5)	0.003(2)	1.18(4)
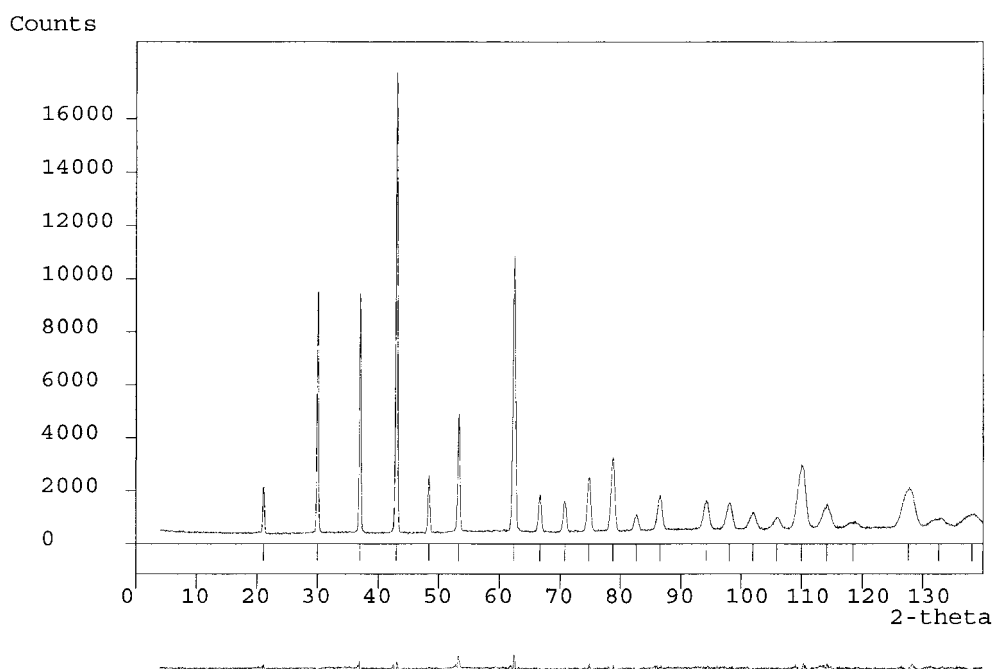
Figure 1. The neutron diffraction pattern obtained at 300 K, indicating the goodness of fit with the pattern calculated from the structural model in table 1.

ordering, with a Néel temperature, T_N, of 155 K [18], the possibility of the extra peaks being due to an ordered magnetic structure was investigated. Thus a double-pattern refinement of the low temperature data was carried out. The magnetic structure (consisting solely of iron ions) was described in terms of a single propagation vector $K = (0, 0, 0)$ and refined in space group $P1$ with doubled cell parameters of 8.0207(2) Å and $\alpha = \beta = \gamma = 89.89(2)°$, the rhombohedral angle. Positional parameters of the iron ions were fixed at [1/4, 1/4, 1/4], [3/4, 1/4, 1/4], [1/4, 3/4, 1/4], [1/4, 1/4, 3/4], [1/4, 3/4, 3/4], [3/4, 1/4, 3/4], [3/4, 3/4, 1/4] and [3/4, 3/4, 3/4], with only the magnetic scattering calculated. A maximum 2θ angle of 70° was adopted, since the magnetic form factor rends negligible magnetic intensities at higher angles. Positional and thermal parameters were
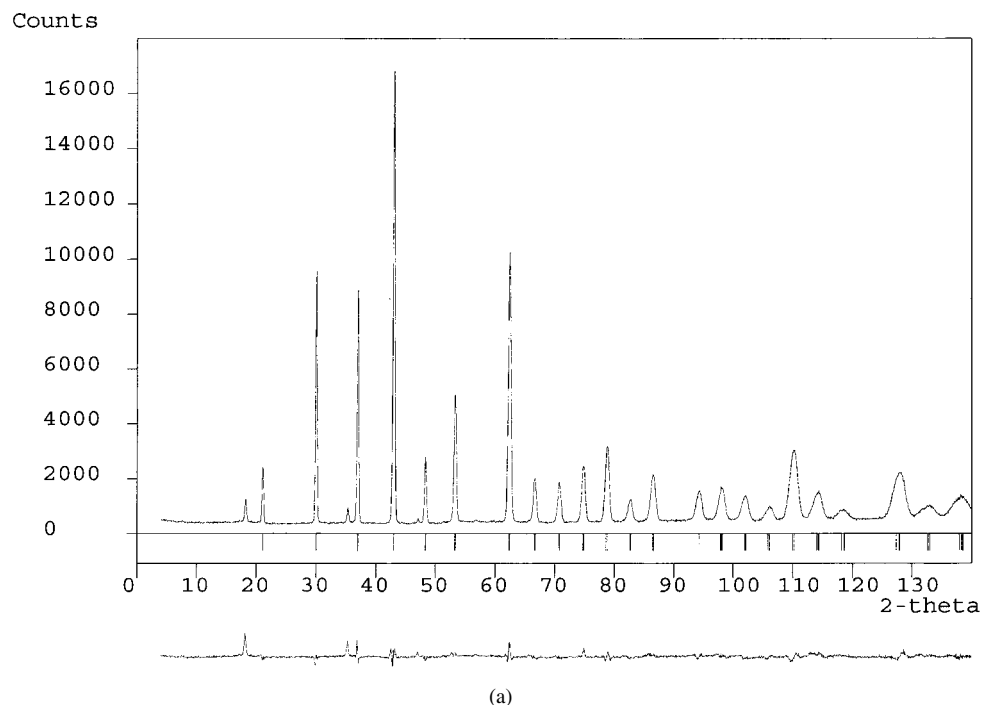
PbFe0.5Nb0.5O3 10K

(a)

Figure 2. The diffraction pattern obtained at 10 K, indicating the goodness of fit obtained (a) by neglecting magnetic moments; and (b) by taking moments into account.

Table 2. Rhombohedral structure of PFN at 10 K with respect to non-doubled rhombohedral (pseudo-cubic) axes: cell parameters in table 3.

Atom	point symmetry	x	y	z	B (Å^2)
Pb	1a	−0.0188(9)	−0.0188(9)	−0.0188(9)	3.02(8)
Nb/Fe	1a	0.5	0.5	0.5	0.07(3)
O	3b	0.5301(5)	0.5301(5)	0.0170(8)	0.69(3)

constrained to be identical in both non-magnetic and magnetic structures, with the magnitudes of the magnetic moments allowed to vary in the magnetic structure. The magnetic R-factor, R_{mag}, was lowest for a simple G-type model with collinear magnetic antiferromagnetic moments of magnitude $|m| = 2.84(6)\ \mu_B$ (figure 3).

The atomic coordinates and isotropic temperature factors obtained from the 10 K refinement are given in table 2. In order to facilitate comprehension, parameters of the non-magnetic structure are quoted both with respect to hexagonal axes (in which the refinement was carried out), and in rhombohedral (pseudo-cubic) axes, which were used for refinement of the magnetic structure. A summary of space groups, cell parameters and R-factors is given in table 3. Uniform reductions in R_p, R_{wp} and R_I factors are observed in passing from the non-magnetic to the magnetic structural solutions, thereby providing strong support for the interpretation that the additional peaks observed at 10 K are due to magnetic, i.e. non-Bragg scattering of the neutrons.
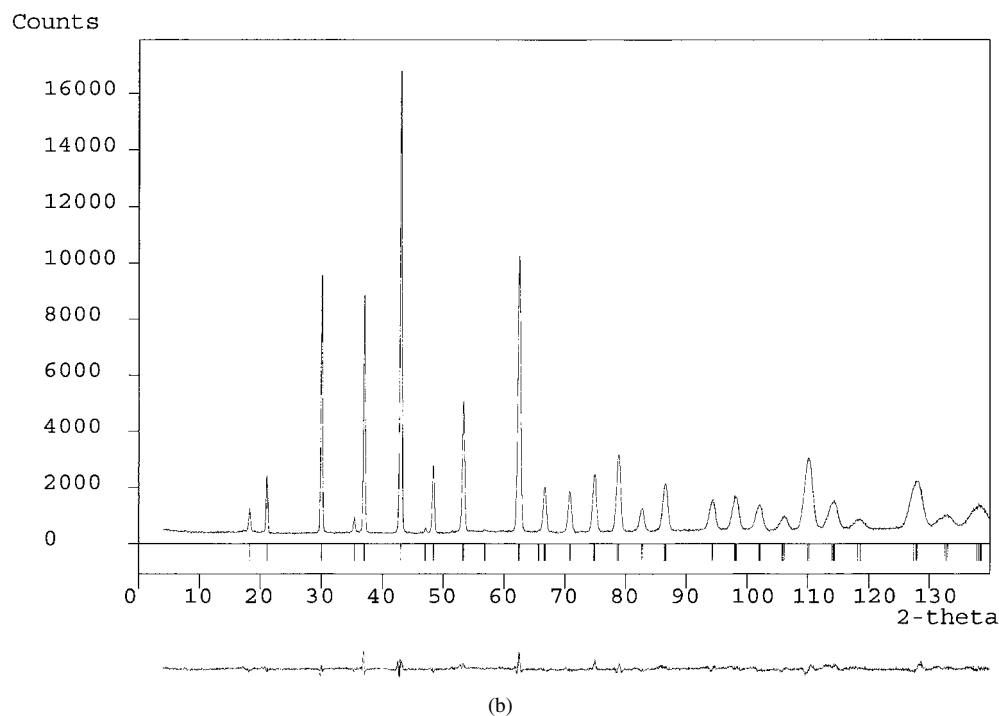
PbFe0.5Nb0.5O3 10K

Counts

(b)

Figure 2. (Continued)

Table 3. Summary of cell parameters and *R*-factors.

T (K)	Axes	*a* (Å)	*c* (Å)	α (°)	R_p	R_{wp}	R_i	R_m
300	Hexagonal	5.6729(4)	6.9493(2)		4.48	5.36	3.63	
	Rhombohedral	4.0123(1)		89.98(2)				
10								
Non-magnetic structure								
	Hexagonal	5.6649(3)	6.9584(2)		6.30	8.46	5.60	
	Rhombohedral	4.0104(1)		89.89(2)				
Magnetic structure								
	Hexagonal	11.3262(2)	13.9160(3)		4.44	5.32	4.06	3.79
	Rhombohedral	8.0207(2)		89.89(2)				

The extent to which this magnitude deviates from the expected (saturation) value of 5.93 μ_B for the $3d^5$ Fe^{3+} ion, which is derived from paramagnetic susceptibility measurements [18], suggests that the simple antiferromagnetic model advocated is only an approximation. Owing to the disorder of Fe^{3+} and Nb^{5+} ions on the B-sites, the strengths of the exchange interactions will vary throughout the crystallites, depending on the local concentrations of diamagnetic Nb^{5+} ions, which will weaken the antiferromagnetic coupling. For example, it is likely that any Fe^{3+} ions in an Nb^{5+}-rich matrix will be very weakly coupled to the magnetic sub-lattice, even at 10 K, leading to a reduction in magnitude of the magnetic moment derived in the refinement which was based on a simple antiferromagnetic model. Thus, on average, it is likely that the antiferromagnetic sub-lattice will not be saturated [19].
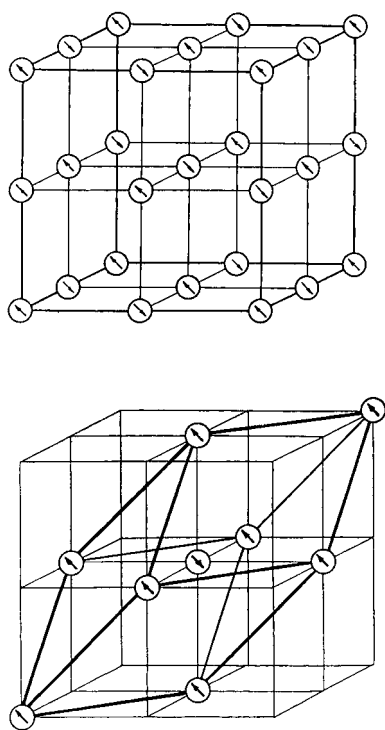
Figure 3. (Top) Schematic representation of the G type of magnetic structure, indicating (bottom) a rhombohedral unit cell with doubled axes.

4. Discussion

In general, the structural parameters obtained for PFN at 300 K are comparable to those found for this compound by x-ray and electron diffraction [20]. It should be noted, however, that the thermal vibrational parameters of the lead ions are large in both the 300 K and the 10 K structures, as has been found in other lead-containing perovskites [21]. As discussed by ourselves in connection with the structure of PMN [22], a literal interpretation that the lead ions (these being the heaviest atoms in the structure) have large vibrational amplitudes is unlikely to be appropriate. It is more likely that there is positional disorder of the lead ions, such that the vector sum of all components of the lead ion displacements perpendicular to the trigonal axis is zero.

Derived parameters describing PbO_{12} and FeO_6/NbO_6 polyhedral volumes, octahedral distortions and ionic displacements along the polar axis are given in table 4. As previously discussed, $R3m$ symmetry dictates that the ratio of the volumes of the AO_{12} and BO_6 octahedra, $V_{Pb}/V_{Fe/Nb}$, is exactly equal to five [23]. As would be expected, $V_{Fe/Nb}$ values are smaller in PFN than their counterparts in $Pb(Mg_{1/3}Nb_{2/3})O_3$ (PMN), where values of 10.975 and 10.957 Å^3 were obtained for $V_{Mg/Nb}$ at 300 K and 10 K, respectively [22]. However, since displacements of the Fe/Nb ions from the centres of their octahedra, $\Delta z_{Fe/Nb}$ are larger than the corresponding $\Delta z_{Mg/Nb}$ values in PMN (9.84 and 14.73 pm at 300 K and 10 K, respectively), the implication is that the FeO_6/NbO_6 octahedra are comparatively more 'oversized' in PFN. This could be regarded as a consequence of the lead ions dictating a minimum PbO_{12} volume, with $V_{Fe/Nb} = V_{Pb}/5$ in $R3m$.

Of particular interest for the PFN compound is the larger value of η (1.002 89, compared to 1.000 16 for PMN) in the 10 K structure, which indicates a significant octahedral (and

Table 4. Crystal structural parameters of the proposed structures of PFN at 300 and 10 K, utilizing the following parameters [23, 24]: V_{Pb} : PbO$_{12}$ polyhedral volume; $V_{Fe/Nb}$:FeO$_6$/NbO$_6$ polyhedral volume; Δs: octahedral distortion perpendicular to trigonal axis; η: octahedral elongation parallel to trigonal axis; Δz_{Pb}, $\Delta z_{Fe/Nb}$: displacements of Pb and Fe/Nb ions parallel to trigonal axis.

Temperature (K)	V_{Pb} (Å^3)	$V_{Fe/Nb}$ (Å^3)	$V_{Pb}/V_{Fe/Nb}$	Δs (pm)	η	Δz_{Pb} (pm)	$\Delta z_{Fe/Nb}$ (pm)
300	53.799	10.760	5	13.33	1.00015	2.34	12.07
10	53.748	10.750	5	7.44	1.00289	31.03	17.92

cuboctahedral) elongation parallel to the polar axis. This is consistent with the large $\Delta z_{Fe/Nb}$ value of 17.92 pm, leading to the expectation that there will be a large electric dipole moment in PFN at 10 K.

Further insight into the structural features of PFN is provided by the Δz_{Pb} and Δs parameters, the latter being a measure of the octahedral distortion perpendicular to the polar axis, which is allowed by rhombohedral symmetry [23]. At 300 K, Δz_{Pb} is smaller than in PMN, which is in agreement with the smaller PbO$_{12}$ polyhedral volume. However, the significant cuboctahedral elongation in PFN at 10 K permits a reversal of this pattern, with a large Δz_{Pb} value of 31.03 pm. This also points to the likelihood of a significant spontaneous polarisation at 10 K. Δs is larger in PFN compared to PMN at 300 K, but smaller at 10 K, the PMN values being 9.31 and 10.24 pm at 300 and 10 K, respectively [22]. The reduction in Δs in cooling PFN from 300 K to 10 K is consistent with the observed increase in octahedral elongation, as the O$_6$ octahedral cage is able to accommodate the B-ions with a smaller degree of distortion.

Finally it is appropriate to comment on the observation of rhombohedral symmetry in our ceramic samples at both 300 K and 10 K, whereas other workers have proposed (with good reason) the existence of monoclinic symmetry in PFN single crystals at room temperature [3]. In our opinion, the macroscopic symmetry obtained is likely to depend on the degree of ordering of Fe^{3+} and Nb^{5+} ions over B-sites: B-site disorder is consistent with rhombohedral symmetry, whereas ordering of Fe^{3+} and Nb^{5+} ions would dictate a reduction of the symmetry to monoclinic. With its 1:1 Fe:Nb stoichiometry, PFN will be susceptible to B-site ordering, although the difference in ionic radii between Fe^{3+} and Nb^{5+} is too small to provide a strong driving force for this. Further work encompassing thermal treatment (e.g. annealing) of PFN ceramics should be fruitful in investigating this question.

Acknowledgments

References

[1] Brunskill I H, Schmid H and Tissot P 1981 *Ferroelectrics* **37** 547
[2] Bokov A A and Emelyanov S M 1991 *Phys. Status Solidi* b **164** K109
[3] Bonny V, Bonin M, Sciau P, Schenk K J and Chapuis G 1997 *Solid State Commun.* **102** 347
[4] Yasuda N and Ueda Y 1989 *Ferroelectrics* **95** 147
[5] Yokosuka M 1993 *Japan. J. Appl. Phys.* **32** 1142
[6] Fu S L and Chen C F 1989 *Ferroelectrics* **82** 119

[7] Smolenskii G A, Agranovskaia A I, Popov S N and Isupov V A 1958 *Sov. Phys.–Tech. Phys.* **3** 1981
[8] Bokov V A, Myl'nikova J E and Smolenskii G A 1962 *Sov. Phys.–JETP* **15** 447
[9] Pietrzak J, Maryanowska A and Leciejewicz J 1981 *Phys. Status Solidi* a **65** K79
[10] Brunskill I H and Schmid H Z 1981 *Ferroelectrics* **37** 547
[11] Ehses K H and Schmid H Z 1983 *Z. Kristallogr.* **162** 64
[12] Kochetkov V V and Venevtsev Y N 1979 *Izv. Akad. Nauk SSSR Neorg. Mater.* **15** 1833
[13] Dulkin E A, Raevskii I P, Emel'yanov S M 1997 *Russ. J. Solid State Phys.* **39** 363
[14] Ananta S and Thomas N W 1999 *J. Eur. Ceram. Soc.* **19** 1873
[15] Ananta S and Thomas N W 1999 *J. Eur. Ceram. Soc.* **19** 155
[16] Rodrigues-Carvajal J 1993 *Physica* B **192** 55
[17] Sears V F 1992 *Neutron News* **3** 28
[18] Maryanowska A and Pietrzak J 1994 *Ferroelectrics* **162** 81
[19] Astrov D N, Al'shin B I, Zorin R V and Drobyshev L A 1969 *Sov. Phys.–JETP* **28** 1123
[20] Platonov G L, Drobyshev L A, Tomashpol'skii Y Y and Venevtsev Y N 1969 *Kristallographia* **14** 800
[21] Kupriyanov M and Kogan V 1991 *Ferroelectrics* **124** 213
[22] Thomas N W, Ivanov S, Ananta S, Tellgren R and Rundlof H 1999 *J. Eur. Ceram. Soc.* **19** 2667
[23] Thomas N W and Beitollahi A 1994 *Acta Crystallogr.* B **50** 549